Hyperfine Interactions **138:** 35–40, 2001.

Observation of the Molecular Quenching of μp(2S) Atoms

R. POHL[1,2,⋆], H. DANIEL[2], F. J. HARTMANN[2], P. HAUSER[2], Y. W. LIU[2], F. KOTTMANN[3], C. MAIERL[2], V. E. MARKUSHIN[1], M. MÜHLBAUER[2], C. PETITJEAN[1], W. SCHOTT[2] and D. TAQQU[1]

[1] *Paul Scherrer Institut, CH-5232 Villigen, Switzerland; e-mail: Randolf.Pohl@psi.ch*
[2] *Physik-Department, Technische Universität München, DE-85747 Garching, Germany*
[3] *Institut für Teilchenphysik, ETH-Hönggerberg, CH-8093 Zürich, Switzerland*

Abstract. Kinetic energy distributions of muonic hydrogen atoms μp(1S) have been obtained by means of a time-of-flight technique for hydrogen gas pressures between 4 and 64 hPa. A high energy component of $\sim$ 900 eV observed in the data is interpreted as the signature of long-lived μp(2S) atoms, which are quenched in a non-radiative process leading to the observed high energy: the collision of a thermalized μp(2S) atom with a hydrogen molecule H_2 results in the resonant formation of a $\{[(pp\mu)^+]^* pee\}^*$ molecule. Then the $(pp\mu)^+$ complex undergoes Coulomb de-excitation and the $\sim$ 1.9 keV excitation energy is shared between a μp(1S) atom and one proton. The preliminary analysis of the time spectra gives a long-lived μp(2S) population of $\sim$ 1% of all stopped muons, and a quenching rate of $\sim 4 \cdot 10^{11}$ s^{-1}.

Key words: exotic atom, muonic hydrogen, 2S state, molecular effects, resonant de-excitation.

1. Introduction

Hydrogen-like atoms have served as very successful probes of the basic aspects of the laws of physics. It is the detailed investigation of the hydrogen atom that led to the development of quantum mechanics, and the discovery of the Lamb shift in 1947 [1] motivated the description of physical processes via quantum field theory. Muonic hydrogen μ^-p has been of interest for a long time since the measurement of the Lamb shift (2S–2P energy difference) could give a precise value for the root mean squared (RMS) charge radius of the proton. Together with the recent advances in hydrogen spectroscopy [2], such an experiment would lead to a test of bound state quantum electrodynamics (QED) on a new level of precision.

The muonic hydrogen Lamb shift experiment [3] is only feasible if a sufficiently large population of long-lived (lifetime $\geqslant$ a few hundred ns) metastable μp(2S) atoms can be produced. All previous experiments taken out to establish the existence of such long-lived metastable atoms did not find any sign of μp(2S)

⋆ Corresponding author.

longevity [4–7]. The present investigation, which has been performed at PSI, is the first observation of long-lived μp(2S) atoms [8].

We have found high-energetic μp(1S) atoms with a kinetic energy of $\sim$ 900 eV. They originate from μp(2S) atoms which are quenched in a collision with a hydrogen molecule H_2. The $\sim$ 1.9 keV excitation energy of the μp(2S) atom is shared between the formed μp(1S) atom and one proton. Momentum conservation implies that the formed μp(1S) atom acquires a kinetic energy of $\sim$ 900 eV. The appearance rate of these high-energetic μp(1S) atoms (i.e., the μp(2S) quenching rate) is rather large and can probably best be explained by the so-called side path mechanism [9], which is the resonant formation of a $\{[(pp\mu)^+]^* pee\}^*$ molecule from the 2S state of μp, and subsequent Coulomb de-excitation of the $(pp\mu)^+$ complex.

The following two sections of this paper explain briefly the experimental setup and the data analysis procedure. The data is presented and discussed in Section 4. In Section 5 we discuss the processes involved in the formation and de-excitation of the $\{[(pp\mu)^+]^* pee\}^*$ molecule.

2. Experiment

The experiment measured the kinetic energy distributions of μp(1S) atoms in gaseous H_2 at 4, 16 and 64 hPa, at 290 K. For a detailed description of the experimental setup see [10].

The principle is to stop low-energy muons on the axis of a cylindrical low-pressure gas target with thin windows, and to measure the time-of-flight (TOF) distribution of the μp atoms traveling in arbitrary directions from the axis to the cylinder wall. The kinetic energy distributions are deduced at each gas pressure from the measured time-of-flight data by means of Monte Carlo simulations. The time-of-flight is given by the time difference between muon stop and arrival of the μp atom at the inner gold-coated surface of the cylinder. The muon is transferred to gold and μAu X-rays of MeV-energies are emitted which are detected in CsI(Tl) crystals surrounding the target ("gold events"). The target is located in a strong axial magnetic field which forces the incoming muons to follow the field lines. This results in an approximately pencil-sized stopping volume. The neutral μp atom is not affected by the magnetic field.

A particular advantage of the cylinder geometry is that a large fraction of the μp(1S) atoms reach the wall along a path length which is only slightly larger than the path perpendicular to the axis. This results in a good velocity resolution. Target diameters of 58 and 20 mm were used for the present analysis. The larger target can resolve kinetic energies of up to 1 keV.

3. Data analysis

For the fit of the measured TOF time spectra we developed a Monte Carlo (MC) simulation to generate a set of time spectra for various kinetic energies for each

pressure and target diameter. The fit function was then a superposition of the different MC time spectra, i.e., we fitted the weights (i.e., amplitudes) of those Monte Carlo generated functions to the measured time spectra. The time spectra taken with 20 and 58 mm target diameter were fitted simultaneously for each gas pressure.

The MC took into account the geometry of the target and the detectors, X-ray detection efficiencies, axial and radial muon stop distributions, and effects of scattering of muonic hydrogen atoms on hydrogen molecules and the gold surface of the target cylinder. The initial population of the μp(1S) atoms was assumed to be statistically distributed between the hyperfine levels F = 0 and F = 1 with 75% of the μp(1S) starting from the F = 1 state, and the evolution of the population of the two hyperfine levels due to inelastic collisions $\mu p(1S,F) + H_2 \rightarrow \mu p(1S,F') + H_2$ was modeled in the simulation, too. The scattering cross sections of Adamczak [11] were used for LAB kinetic energies below 9 eV, which corresponds roughly to the ionization energy (breakup) of the H_2 molecule. Between 9 eV and 1000 eV cross sections calculated by Cohen [12] were used.

The set of MC generated time spectra used in the analysis of each measured TOF time spectrum included a "continuum" of kinetic energies below 64 eV (similar to [10]), plus some Coulomb-deexcitation delta energies ($6 \rightarrow 5$ at 14.6 eV, $5 \rightarrow 4$ at 26.9 eV, $4 \rightarrow 3$ and $5 \rightarrow 3$ at 58.2 and 85.2 eV, respectively, and $3 \rightarrow 2$ at 166.3 eV) and a 898.1 eV component representing the quenched μp(2S) atoms. The MC time spectrum of this last component was convoluted with a lifetime $\tau_{2S} = 1/\lambda^{2S}_{quench}$, and the amplitude assigned to that spectrum was $A_{2S} = R_{2S}\lambda^{2S}_{quench}$, where R_{2S} is the fraction of long-lived μp(2S) atoms (normalized to all μp atoms). A time offset Δt_{2S} of this 2S-signal was introduced which can be understood as a "thermalization" time of the μp(2S) atoms. This time offset accounts for the fact that the μp(2S) atoms are formed at high kinetic energies, but they have to decelerate in elastic collisions with H_2 molecules before the resonant formation of $\{[(pp\mu)^+]^* pee\}^*$ molecules can occur.

4. Measured TOF spectra

Especially at 64 and 16 hPa, the early parts of the time spectra taken in the 58 mm target (the one with the largest sensitivity to high kinetic energies) show a distinct peak originating from very high energetic μp(1S) atoms (Figure 1).

First the data sets at 64 and 16 hPa were analysed independently of each other. Lifetime τ_{2S}, amplitude A_{2S} and time offset Δt_{2S} of the 2S-signal were fitted freely, as were the amplitudes of the continuum and Coulomb de-excitation contributions. The lifetime τ_{2S} shows an excellent agreement for the two spectra at 64 and 16 hPa: it scales as the inverse of the pressure. This proves that the observed signal is not a result of "ordinary" Coulomb de-excitation $n = 2 \rightarrow 1$ which takes place during the prompt cascade. In that case, no additional lifetime τ_{2S} would be observable ($\tau_{2S} = 0$), and the shape of the signal would only depend on the target geometry

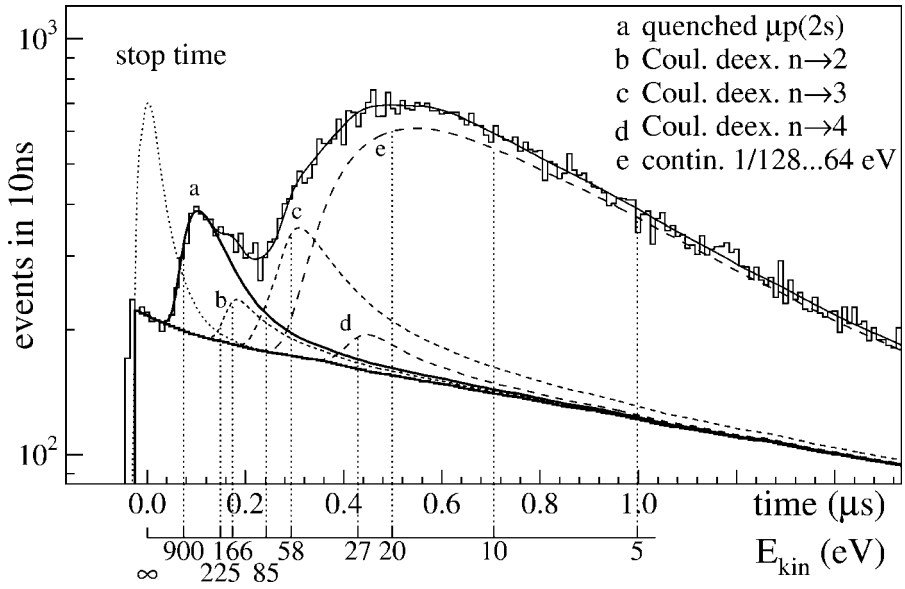

Figure 1. TOF spectrum taken at 64 mbar H_2 pressure in the 58 mm diameter target. The high-energetic μp(1S) component originating from quenched μp(2S) is clearly visible. This μp(2S) signal (a) is convoluted with a (fitted) lifetime. The fit also contains some discrete high energies from low-n Coulomb de-excitation (b,c,d) , and a "continuum"-energy distribution of energies between 1/128 eV and 64 eV (e). Background and stop time distribution (dashed peak) have been measured. Note the kinetic energy scale for the TOF in the 58 mm diameter target.

which was the same for the different pressures. Instead, the fact that the lifetime scales as the inverse of the pressure shows that the μp(2S) atoms are indeed "long-lived" and diffuse in the H_2 target gas experiencing collisions with H_2 atoms until they eventually undergo de-excitation giving the μp(1S) atoms with $\sim$ 900 eV kinetic energy. The data can not be fitted assuming $\tau_{2S} = 0$.

At 4 hPa the 2S-signal is too weak to be treated in a completely free fit. Lifetime and population are highly correlated in a way that a longer lifetime requires a larger population to explain the number of measured events.

The combined analysis of the data at 4, 16 and 64 hPa gives a preliminary value for the μp(2S) quenching rate of $\lambda^{2S}_{\rm quench} \approx 4 \cdot 10^{11}$ s^{-1} at liquid hydrogen density (LHD). The long-lived μp(2S) population we deduce is slightly higher than 1% of all stopped muons at 4, 16, and 64 hPa.

5. Molecule formation and de-excitation

The well-known Vesman mechanism [13] has been shown to be the path through which muon-catalyzed dt fusion proceeds. This process of muonic molecule formation can also take place from excited states [14–19].

The process leading to the observed fast non-radiative de-excitation of μp(2S) atoms is believed to proceed predominantly via the following series of steps:

In a thermal collision between a μp(2S) atom with a hydrogen molecule H_2 a molecule $\{[(pp\mu)^+]^* pee\}^*$ is formed. Rotational and vibrational excitations of the formed electronic molecule $\{[(pp\mu)^+]^* pee\}^*$ can absorb the small excess energy from the formation of the muonic molecule $(pp\mu)^+$:

$$\mu p(2S) + H_2 \rightarrow \{[(pp\mu)^+]^* pee\}^*. \quad (1)$$

The existence of Feshbach-type three-body resonances in the formation of the $(pp\mu)^+$ "pseudonucleus" enhances the formation of the H_2-like electronic molecule significantly. Recent calculations [9, 20] show that there exists a series of resonance states below the $p + \mu p(n = 2)$ dissociation limit, which leads to a very efficient formation of the weakly bound molecule $\{[(pp\mu)^+]^* pee\}^*$.

Subsequent Auger decay to states with a binding energy of $\geqslant$ 16 eV can then stabilize the molecule against back-decay.

Finally, the $[(pp\mu)^+]^*$ undergoes Coulomb decay into $\mu p(1S) + p +$ kin. energy leaving the second p or H as a spectator. The rates for this process are quite large, because the resonance states below the $p + \mu p(2S)$ state are embedded in the continuum above the dissociation limit $p + \mu p(1S)$ [15].

The rates of molecular formation have not been calculated yet. In any case, at low gas pressures they are by orders of magnitude smaller than the subsequent Auger, Coulomb or Stark decay rates. The measured μp(2S) quenching rate λ^{2S}_{quench} is therefore practically equal to the molecular formation rate.

6. Conclusions

We have observed μp(1S) atoms with a kinetic energy of $\sim$ 900 eV which are produced when thermalized μp(2S) atoms are quenched in a collision with a H_2 molecule. We preliminarily deduce a long-lived μp(2S) population of $\sim$ 1% of all muons, and a non-radiative quenching rate for thermalized μp(2S) atoms of $\sim 4 \cdot 10^{11}$ s^{-1} at LHD. The large value of this quenching rate can probably best be explained assuming a resonant formation of $\{[(pp\mu)^+]^* pee\}^*$ molecules from the 2S state of μp followed by a stabilizing Auger decay and subsequent Coulomb dissociation to high-energetic μp(1S) atoms.

Acknowledgements

The authors would like to thank A. Adamczak, J. S. Cohen and V. S. Melezhik for providing us with cross sections, and J. Wallenius and T. Jensen for fruitful discussions.

References

1. Lamb, Jr., W. E. and Retherford, R. C., *Phys. Rev.* **72** (1947), 241.
2. de Beauvoir, B. *et al.*, *Eur. Phys. J. D* **12** (2000), 61.

3. Kottmann, F. *et al.*, *Hyp. Interact.*, this issue.
4. Anderhub, H. *et al.*, *Phys. Lett. B* **71** (1977), 443.
5. Egan, P. O. *et al.*, *Phys. Rev. A* **23** (1981), 1152.
6. Böcklin, J., Ph.D. thesis, ETH Zürich No. 7161 (1982) (unpublished).
7. Anderhub, H. *et al.*, *Phys. Lett. B* **143** (1984), 65.
8. Pohl, R., Ph.D. thesis, ETH Zürich No. 14096 (2001) (unpublished).
9. Wallenius, J. *et al.*, *Hyp. Interact.*, this issue.
10. Kottmann, F. *et al.*, *Hyp. Interact.* **119** (1999), 3.
11. Adamczak, A. *et al.*, *At. Data and Nucl. Data Tables* **62** (1996), 255; Adamczak, A., *Hyp. Interact.* **101/102** (1996), 113; Adamczak, A. *et al.*, *Hyp. Interact.* **82** (1993), 91.
12. Cohen, J. S. and Struensee, M. C., *Phys. Rev. A* **43** (1991), 3460; Cohen, J. S., *Phys. Rev. A* **43** (1991), 4668; Cohen, J. S., *Phys. Rev. A* **44** (1991), 2836; Cohen, J. S., private communication.
13. Vesman, E. A., *Pis'ma Zh. Eksp. Teor. Fiz.* **5** (1967), 113 [*JETP Lett.* **5** (1967), 91].
14. Hara, S. and Ishihara, T., *Phys. Rev. A* **40** (1989), 4232.
15. Shimamura, I., *Phys. Rev. A* **40** (1989), 4863.
16. Hu, C. Y. and Bhatia, A. K., *Phys. Rev. A* **43** (1991), 1229.
17. Froelich, P. and Wallenius, J., *Phys. Rev. Lett.* **75** (1995), 2108.
18. Wallenius, J. and Froelich, P., *Phys. Rev. A* **54** (1996), 1171.
19. Jonsell, S., Wallenius, J. and Froelich, P., *Phys. Rev. A* **59** (1999), 3440.
20. Hilico, L., private communication.